Supplemental Material: Angular dynamics of non-spherical particles settling in turbulence

K. Gustavsson,[1] J. Jucha,[2,3] A. Naso,[4] E. Lévêque,[4] A. Pumir,[2] and B. Mehlig[1]

[1]*Department of Physics, Gothenburg University, 41296 Gothenburg, Sweden*
[2]*Laboratoire de Physique, Ecole Normale Supérieure de Lyon and CNRS, F-69007, Lyon, France*
[3]*Projektträger Jülich, Forschungszentrum Jülich GmbH, D-52425, Germany*
[4]*LMFA, Ecole Centrale de Lyon and CNRS, F-69134, Ecully, France*

PACS numbers: 05.40.-a,47.55.Kf,47.27.eb

I. DETAILS ON EQUATIONS OF MOTION

We begin by recalling the form of the resistance tensors, defined by Eq. (2) in the main text. The tensor $\mathbb{M}^{(t)}$ relates the force on the particle to the slip velocity, the difference between the fluid and the particle velocities. The superscript refers to the translational (t) degrees of freedom. The tensor is expressed as:

$$M_{ij}^{(t)} \equiv C_{\perp}^{(t)}\delta_{ij} + (C_{\parallel}^{(t)} - C_{\perp}^{(t)})n_i n_j\,. \tag{S1}$$

For the rotational degrees of freedom, superscript (r), the resistance tensor is decomposed into two terms, $\mathbb{M}^{(r1)}$ and $\mathbb{M}^{(r2)}$. The first term relates the torque to the angular slip velocity, the difference between the rotation rate of the fluid and that of the particle. The second term relates the torque to the local strain in the fluid. The expression for $\mathbb{M}^{(r1)}$ is similar to Eq. (S1):

$$M_{ij}^{(r1)} \equiv K_{\perp}^{(r1)}\delta_{ij} + (K_{\parallel}^{(r1)} - K_{\perp}^{(r1)})n_i n_j\,. \tag{S2}$$

The expression for $\mathbb{M}^{(r2)}$ is of the form:

$$M_{ijk}^{(r2)} = K^{(r2)}\epsilon_{ijl}n_k n_l\,. \tag{S3}$$

Here ϵ_{ijl} is the completely anti-symmetric Levi-Civita tensor, and the summation convention is used: repeated indices are summed from 1 to 3. The forms of the tensors in Eqs. (S1), (S2), and (S3) follow from the symmetry properties of axisymmetric particles. For spheroidal particles, the coefficients in Eqs. (S1), (S2), and (S3) are known [1]:

$$C_{\perp}^{(t)} = \frac{8(\lambda^2-1)}{3\lambda((2\lambda^2-3)\beta+1)}\,,\quad C_{\parallel}^{(t)} = \frac{4(\lambda^2-1)}{3\lambda((2\lambda^2-1)\beta-1)}\,, \tag{S4a}$$

$$K_{\perp}^{(r1)} = \frac{8a_{\parallel}a_{\perp}(\lambda^4-1)}{9\lambda^2((2\lambda^2-1)\beta-1)}\,,\quad K_{\parallel}^{(r1)} = -\frac{8a_{\parallel}a_{\perp}(\lambda^2-1)}{9(\beta-1)\lambda^2}\,, \tag{S4b}$$

$$K^{(r2)} = -K_{\perp}^{(r1)}\frac{\lambda^2-1}{\lambda^2+1}\,,\quad \beta = \frac{\ln[\lambda+\sqrt{\lambda^2-1}]}{\lambda\sqrt{\lambda^2-1}}\,. \tag{S4c}$$

Here $\lambda \equiv a_{\parallel}/a_{\perp}$ is the aspect ratio of the spheroid, $2a_{\parallel}$ is the length of the particle symmetry axis, and $2a_{\perp}$ is the particle diameter. Prolate spheroids have $\lambda > 1$. Oblate spheroids correspond to $\lambda < 1$. In this case, Eq. (S4c) reduces to $\beta = \arccos(\lambda)/[\lambda\sqrt{1-\lambda^2}]$. The motion of the particle is fully characterised by the knowledge of the velocity of the particle, $\boldsymbol{v}$, and the angular velocity of the particle in the laboratory frame, $\boldsymbol{\omega}$. The direction of the particle symmetry vector, $\boldsymbol{n}$, is related to the angular velocity $\boldsymbol{\omega}$ by the kinematic equation:

$$\frac{\mathrm{d}\boldsymbol{n}}{\mathrm{d}t} = \boldsymbol{\omega}\wedge\boldsymbol{n}\,. \tag{S5}$$

The equation for the angular velocity reads in the laboratory frame:

$$\frac{\mathrm{d}}{\mathrm{d}t}\big(\mathbb{J}(\boldsymbol{n})\boldsymbol{\omega}\big) = \boldsymbol{T}\,. \tag{S6}$$

Here $\boldsymbol{T}$ is the torque on the particle, and $\mathbb{J}(\boldsymbol{n})$ is the inertia tensor of the particle. For a spheroid its elements are [1]

$$J_{ij}(\boldsymbol{n}) = \frac{ma_{\perp}^2}{5}\left[(1+\lambda^2)\delta_{ij} + (1-\lambda^2)n_i n_j\right]\,. \tag{S7}$$

A difficulty is that the inertia tensor depends on the instantaneous orientation $\boldsymbol{n}(t)$. In the DNS we therefore express Eq. (S6) in the particle frame, at the cost of an extra term in the equations of motion, due to the rotation of the axes [2].

II. DETAILS ON DIRECT NUMERICAL SIMULATIONS OF TURBULENCE

A. Method of resolution

The Navier-Stokes equations read:

$$\rho_f[\partial_t \boldsymbol{u} + (\boldsymbol{u}\cdot\nabla)\boldsymbol{u}] = -\nabla p + \nu\rho_{\rm f}\nabla^2\boldsymbol{u} + \boldsymbol{\Phi} \tag{S8}$$

where $\boldsymbol{u}$ is the velocity field of the flow, which is assumed to be incompressible:

$$\nabla\cdot\boldsymbol{u} = 0\,, \tag{S9}$$

p is the pressure field, $\boldsymbol{\Phi}$ is a forcing term, ρ_f is the density of the fluid, and ν is the kinematic viscosity. The equations are solved in a triply periodic domain of size L^3, using a pseudo-spectral method. The code has been described elsewhere [3]. Briefly, the fluid is forced in the band of lowest wave-numbers by imposing an energy injection of ε. The values of ε chosen here correspond to cloud conditions, see subsection II B. The Kolmogorov length, $\eta_{\rm K} = (\nu^3/\varepsilon)^{1/4}$ is of the order of the grid spacing. The code is fully dealiased, using the 2/3-rule [4]. This consists, in practice, in computing the nonlinear term by using only Fourier modes n in the range $0 \le n \le N/3$, where N is the number of grid points in each direction.

The equation of motion of the particles is implemented by interpolating the velocity and velocity gradients at the location of the particle, using tri-cubic schemes. The method has been carefully checked, by systematically comparing the results in the absence of fluid motion $\boldsymbol{u} = 0$, for the code, and for an elementary solver (Mathematica) of the equations of motion of the particle.

B. Choice of parameters

The values chosen in this study correspond to cloud conditions [5]. In physical units, the viscosity chosen here is $\nu = 0.113{\rm cm}^2/{\rm s}$. The number of grid points taken here was $N = 384$, with an energy injection rate of $\varepsilon \approx 1\,{\rm cm}^2/{\rm s}^3$, $N = 784$ ($\varepsilon \approx 16\,{\rm cm}^2/{\rm s}^3$), and $N = 1568$ ($\varepsilon \approx 256\,{\rm cm}^2/{\rm s}^3$). With the values of the parameters chosen here, the size L of the box is equal to 8π cm.

III. DEPENDENCE OF ORIENTATIONAL BIAS ON THE REYNOLDS NUMBER

Fig. S1 shows a comparison between DNS simulations and the statistical model for the orientational bias in flows with different Reynolds numbers: ${\rm Re}_\lambda = 56$ ($\varepsilon = 1\,{\rm cm}^2{\rm s}^{-3}$, ◀), ${\rm Re}_\lambda = 95$ ($\varepsilon = 16\,{\rm cm}^2{\rm s}^{-3}$, •), ${\rm Re}_\lambda = 151$ ($\varepsilon = 256\,{\rm cm}^2{\rm s}^{-3}$, ▼). The DNS data is compared to statistical-model simulations with large Ku. The statistical-model parameters St, and F are determined by the relations to the DNS parameters ${\rm Re}_\lambda$, ${\rm St}_{\rm K}$, and $F_{\rm K}$ described in the main text. The agreement is equally good as that observed in Fig. 1 in the main text.

IV. DETAILS ON THE STATISTICAL MODEL

In the simulations of the statistical model the smooth, incompressible, homogeneous, isotropic, three-dimensional velocity field is given by $\boldsymbol{u} = \boldsymbol{\nabla}\wedge\boldsymbol{\Psi}/\sqrt{6}$, where $\boldsymbol{\Psi}$ is a vector potential [6]. Each component of $\boldsymbol{\Psi}$ consists of a spatial superposition of Fourier modes with random time-dependent prefactors. The statistics of the prefactors is chosen such that the components $\Psi_i(\boldsymbol{x},t)$ are Gaussian distributed with correlation functions

$$\langle\Psi_i(\boldsymbol{x},t)\Psi_j(\boldsymbol{x}',t')\rangle = \delta_{ij}\ell^2 u_0^2 \exp\left[-\frac{|\boldsymbol{x}-\boldsymbol{x}'|^2}{2\ell^2} - \frac{|t-t'|}{\tau}\right], \tag{S10}$$

where $\langle\ldots\rangle$ denotes an ensemble average. We choose the velocity scale as the rms speed of the flow, $u_0 \equiv \sqrt{\langle|\boldsymbol{u}|^2\rangle}$. The correlation length ℓ and correlation time τ are the scales at which Eq. (S10) decay in space and in time. These Eulerian scales constitute the Kubo number ${\rm Ku} = u_0\tau/\eta$ [6].

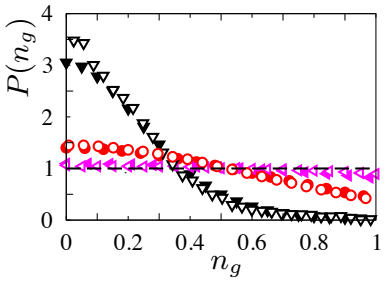

FIG. S1: Orientational bias of spheroids with aspect ratio $\lambda = 1/50$ settling in turbulence. Distribution $P(n_g)$ of $n_g \equiv |\boldsymbol{n}\cdot\hat{\boldsymbol{g}}|$, where $\boldsymbol{n}$ is the particle symmetry-vector and $\hat{\boldsymbol{g}}$ is the direction of gravity. DNS results for $P(n_g)$ with parameters $\mathrm{Re}_\lambda = 56$, $F_\mathrm{K} \approx 570$, $\mathrm{St}_\mathrm{K} \approx 0.02$ (▼); $\mathrm{Re}_\lambda = 95$, $F_\mathrm{K} \approx 70$, $\mathrm{St}_\mathrm{K} \approx 0.08$ (●); and $\mathrm{Re}_\lambda = 151$, $F_\mathrm{K} \approx 9$, $\mathrm{St}_\mathrm{K} \approx 0.32$ (◀). Statistical-model simulations ($\mathrm{Ku} = 10$), as described in the text, open symbols. The isotropic distribution $P(n_g) = 1$ is shown as a dashed line.

V. DETAILS ON THE PERTURBATION THEORY FOR SMALL VALUES OF Ku

A. Implicit solution of equations of motion

We follow the method outlined in Ref. [6] and expand the solution of the equations of motion for the settling spheroid, Eqs. (1) and (2) in the main article, in powers of Ku:

$$\begin{aligned}
\boldsymbol{v}(t) &= \sum_{n=0}^{\infty}(-1)^n\,\mathrm{Ku}^n \int_0^t \mathrm{d}t_1 e^{\mathbb{M}_0^{(t)}(t_1-t)}\Delta\mathbb{M}^{(t)}(t_1)\cdots\int_0^{t_{n-1}}\mathrm{d}t_n e^{\mathbb{M}_0^{(t)}(t_n-t_{n-1})}\Delta\mathbb{M}^{(t)}(t_n)\int_0^{t_n}\mathrm{d}t_{n+1}e^{\mathbb{M}_0^{(t)}(t_{n+1}-t_n)}\\
&\qquad\times\left[\mathrm{F}\hat{\boldsymbol{g}}+\mathbb{M}^{(t)}(t_{n+1})\boldsymbol{u}(\boldsymbol{x}(t_{n+1}),t_{n+1})\right]\\
\boldsymbol{\omega}(t) &= \sum_{n=0}^{\infty}(-1)^n\,\mathrm{Ku}^n \int_0^t \mathrm{d}t_1 e^{\mathbb{M}_0^{(r)}(t_1-t)}\Delta\mathbb{M}^{(r)}(t_1)\cdots\int_0^{t_{n-1}}\mathrm{d}t_n e^{\mathbb{M}_0^{(r)}(t_n-t_{n-1})}\Delta\mathbb{M}^{(r)}(t_n)\int_0^{t_n}\mathrm{d}t_{n+1}e^{\mathbb{M}_0^{(r)}(t_{n+1}-t_n)}\\
&\qquad\times\left[\tfrac{1}{2}\mathbb{M}^{(r)}(t_{n+1})\boldsymbol{\Omega}(\boldsymbol{x}(t_{n+1}),t_{n+1})-\Lambda C_\perp^{(r1)}(\mathbb{S}(\boldsymbol{x}(t_{n+1}),t_{n+1})\boldsymbol{n}(t_{n+1}))\wedge\boldsymbol{n}(t_{n+1})\right.\\
&\qquad\qquad\left.+\,\mathrm{Ku}\,\Lambda(\boldsymbol{\omega}(t_{n+1})\wedge\boldsymbol{n}(t_{n+1}))(\boldsymbol{n}(t_{n+1})\cdot\boldsymbol{\omega}(t_{n+1}))\right]\\
\boldsymbol{n}(t) &= \boldsymbol{n}_0+\mathrm{Ku}\int_0^t\mathrm{d}t_1\boldsymbol{\omega}(t_1)\wedge\boldsymbol{n}(t_1)\,.
\end{aligned}\tag{S11}$$

Here $\Lambda \equiv (\lambda^2-1)/(\lambda^2+1)$, $C_\perp^{(r1)} \equiv 5K_\perp^{(r1)}/(a_\parallel^2+a_\perp^2)$, and we have decomposed the translational resistance tensor into a part that does not depend on the Kubo number, and a Ku-dependent part, $\mathbb{M}^{(t)} = \mathbb{M}_0^{(t)} + \mathrm{Ku}\,\Delta\mathbb{M}^{(t)}$, with

$$\mathbb{M}_0^{(t)} = \mathbb{I}C_\perp^{(t)} + \boldsymbol{n}_0\boldsymbol{n}_0^\mathsf{T}(C_\parallel^{(t)}-C_\perp^{(t)}) \quad\text{and}\quad \Delta\mathbb{M}^{(t)} = [\Delta\boldsymbol{n}\,\boldsymbol{n}_0^\mathsf{T}+\boldsymbol{n}_0\,\Delta\boldsymbol{n}^\mathsf{T}+\mathrm{Ku}\,\Delta\boldsymbol{n}\,\Delta\boldsymbol{n}^\mathsf{T}](C_\parallel^{(t)}-C_\perp^{(t)})\,. \tag{S12}$$

Here $\Delta\boldsymbol{n}$ is a rescaled orientation displacement vector

$$\Delta\boldsymbol{n}(t) \equiv \frac{\boldsymbol{n}(t)-\boldsymbol{n}_0}{\mathrm{Ku}} = \int_0^t \mathrm{d}t_1\boldsymbol{\omega}(t_1)\wedge\boldsymbol{n}(t_1)\,. \tag{S13}$$

The rotational resistance tensors are decomposed in a similar way. Eq. (S11) is an exact, but implicit, solution to Eqs. (1) and (2) in the main article, provided that the initial conditions of the particle velocity and angular velocity are set to zero. The solution (S11) depends implicitly on orientation $\boldsymbol{n}$, the angular velocity $\boldsymbol{\omega}$, and on the centre-of-mass position $\boldsymbol{x}$ of the particle. If the Kubo number is small we can terminate the solution (S11) at some order in Ku and solve the resulting set of equations iteratively. Details are given in Ref. [6].

B. Explicit solution of equations of motion for small values of Ku

To eliminate the implicit dependence on $\boldsymbol{x}$ through the flow velocity $\boldsymbol{u}(\boldsymbol{x}(t),t)$ and through the flow velocity gradients $\mathbb{A}(\boldsymbol{x}(t),t)$, we consider a decomposition of particle trajectories $\boldsymbol{x}(t)$ into two parts:

$$\boldsymbol{x}(t) \equiv \boldsymbol{x}^{(\mathrm{d})}(t) + \delta\boldsymbol{x}(t)\,. \tag{S14}$$

The first part, $\boldsymbol{x}^{(\mathrm{d})}(t)$, is a deterministic part that is obtained by setting the turbulent velocity $\boldsymbol{u}$ to zero in the particle equation of motion. The second part is the remainder, the flow-dependent fluctuating part, $\delta\boldsymbol{x}(t) \equiv \boldsymbol{x}(t) - \boldsymbol{x}^{(\mathrm{d})}(t)$. The deterministic part of the trajectory is obtained by integrating the solution for the particle velocity in Eq. (S11) with $\boldsymbol{u} = 0$ and $\mathbb{A} = 0$. For large values of t, the corresponding particle velocity approaches the settling velocity $\boldsymbol{v}_{\mathrm{s}}(\boldsymbol{n}_0)$ in a quiescent fluid (Eq. (4) in the main text)

$$\boldsymbol{v}_{\mathrm{s}}(\boldsymbol{n}_0) = \mathrm{F\ St}\,[\mathbb{M}^{(t)}(\boldsymbol{n}_0)]^{-1}\hat{\boldsymbol{g}} = \mathrm{F\ St}\Big[\frac{\mathbb{I}}{C_\perp^{(t)}} + \frac{\boldsymbol{n}_0\boldsymbol{n}_0^{\mathsf{T}}}{C_\parallel^{(t)}} - \frac{\boldsymbol{n}_0\boldsymbol{n}_0^{\mathsf{T}}}{C_\perp^{(t)}}\Big]\hat{\boldsymbol{g}}\,. \tag{S15}$$

The corresponding deterministic trajectory approaches the form $\boldsymbol{x}^{(\mathrm{d})}(t) = \boldsymbol{x}_0 + \boldsymbol{v}_{\mathrm{s}}(\boldsymbol{n}_0)t$ at large times. Here $\boldsymbol{n}_0$ is the constant orientation at which the particle settles. In the steady state, the orientation $\boldsymbol{n}_0$ must be chosen from a stationary distribution of particle orientations that must be determined self consistently.

For small values of Ku, the flow gives rise to small deviations $\delta\boldsymbol{x}$ from the deterministic settling trajectories $\boldsymbol{x}^{(\mathrm{d})}$. Following the procedure outlined in Ref. [6], we attempt a series expansion of the fluid velocity experienced by particles in terms of small $\delta\boldsymbol{x}$

$$\boldsymbol{u}(\boldsymbol{x}(t),t) = \boldsymbol{u}(\boldsymbol{x}^{(\mathrm{d})}(t),t) + \delta\boldsymbol{x}^{\mathsf{T}}(t)\boldsymbol{\nabla}\boldsymbol{u}(\boldsymbol{x}^{(\mathrm{d})}(t),t) + \dots\,, \tag{S16}$$

and similarly for the fluid-velocity gradients. We insert these expansions into the implicit solutions (S11), and iterate the solution to find an expression for the orientation $\boldsymbol{n}$ valid for small values of Ku. To second order in Ku we find Eq. (3) in the main article. Writing out all terms explicitly this equation reads in vector notation:

$$\begin{aligned}
\boldsymbol{n}(t) = \boldsymbol{n}_0 &+ \mathrm{Ku}\int_0^t \mathrm{d}s\,[1 - e^{(s-t)C_\perp^{(r1)}/\,\mathrm{St}}]\;(\delta\boldsymbol{x}_s\cdot\boldsymbol{\nabla})\big\{\mathbb{O}(\boldsymbol{x},s)\boldsymbol{n}_0 + \tfrac{\lambda^2-1}{\lambda^2+1}\big[\mathbb{S}(\boldsymbol{x},s)\boldsymbol{n}_0 - \big(\boldsymbol{n}_0\cdot\mathbb{S}(\boldsymbol{x},s)\boldsymbol{n}_0\big)\boldsymbol{n}_0\big]\big\}\Big|_{\boldsymbol{x}=\boldsymbol{x}_s^{(\mathrm{d})}} \\
&+ \mathrm{Ku}\int_0^t \mathrm{d}s(1 - e^{C_\perp^{(r1)}(s-t)/\,\mathrm{St}})[\mathbb{O}_s\boldsymbol{n}_0 + \Lambda(\mathbb{S}_s\boldsymbol{n}_0 - (\boldsymbol{n}_0^{\mathsf{T}}\mathbb{S}_s\boldsymbol{n}_0)\boldsymbol{n}_0)] \\
&+ \mathrm{Ku}^2\int_0^t \mathrm{d}t_1\int_0^{t_1}\mathrm{d}t_2\Big[d_1\boldsymbol{n}_0^{\mathsf{T}}\mathbb{O}_{t_1}\mathbb{O}_{t_2} + d_2(\boldsymbol{n}_0^{\mathsf{T}}\mathbb{O}_{t_1}\mathbb{O}_{t_2}\boldsymbol{n}_0)\boldsymbol{n}_0 + d_3(\boldsymbol{n}_0^{\mathsf{T}}\mathbb{O}_{t_1}\mathbb{S}_{t_2}\boldsymbol{n}_0)\boldsymbol{n}_0 + d_4(\boldsymbol{n}_0\mathbb{S}_{t_1}\boldsymbol{n}_0)(\boldsymbol{n}_0\mathbb{S}_{t_2}\boldsymbol{n}_0)\boldsymbol{n}_0 \\
&+ d_5\mathbb{O}(t_2)\mathbb{S}(t_1)\boldsymbol{n}_0 + d_6(\boldsymbol{n}_0^{\mathsf{T}}\mathbb{S}_{t_1}\mathbb{O}_{t_2}\boldsymbol{n}_0)\boldsymbol{n}_0 + d_7(\boldsymbol{n}_0^{\mathsf{T}}\mathbb{S}_{t_1}\mathbb{S}_{t_2}\boldsymbol{n}_0)\boldsymbol{n}_0 + d_8(\boldsymbol{n}_0\mathbb{S}_{t_2}\boldsymbol{n}_0)\mathbb{O}_{t_1}\boldsymbol{n}_0 + d_9(\boldsymbol{n}_0\mathbb{S}_{t_1}\boldsymbol{n}_0)\mathbb{O}_{t_2}\boldsymbol{n}_0 \\
&+ d_{10}\mathbb{O}_{t_1}\mathbb{O}_{t_2}\boldsymbol{n}_0 + d_{11}\mathbb{O}_{t_1}\mathbb{S}_{t_2}\boldsymbol{n}_0 + d_{12}(\boldsymbol{n}_0\mathbb{S}_{t_2}\boldsymbol{n}_0)\mathbb{S}_{t_1}\boldsymbol{n}_0 + d_{13}(\boldsymbol{n}_0\mathbb{S}_{t_1}\boldsymbol{n}_0)\mathbb{S}_{t_2}\boldsymbol{n}_0 + d_{14}\mathbb{S}_{t_1}\mathbb{O}_{t_2}\boldsymbol{n}_0 + d_{15}\mathbb{S}_{t_1}\mathbb{S}_{t_2}\boldsymbol{n}_0\Big]
\end{aligned} \tag{S17}$$

with $\mathbb{O}_t \equiv \mathbb{O}(\boldsymbol{x}_t^{(\mathrm{d})},t)$, $\mathbb{S}_t \equiv \mathbb{S}(\boldsymbol{x}_t^{(\mathrm{d})},t)$. The coefficients are:

$$\begin{aligned}
d_1 &= -\frac{C_\perp^{(r1)}(\Lambda-1)e^{C_\perp^{(r1)}(t_1-t)/\,\mathrm{St}+C_\parallel^{(r1)}(t_2-t)/\,\mathrm{St}}}{C_\perp^{(r1)}+C_\parallel^{(r1)}} + (\Lambda-1)e^{C_\perp^{(r1)}(t_1-t)/\,\mathrm{St}+C_\parallel^{(r1)}(t_2-t_1)/\,\mathrm{St}} - \frac{C_\parallel^{(r1)}(\Lambda-1)e^{C_\parallel^{(r1)}(t_2-t_1)/\,\mathrm{St}}}{C_\perp^{(r1)}+C_\parallel^{(r1)}} \\
d_2 &= (1-\Lambda)e^{C_\perp^{(r1)}(t_1-t)/\,\mathrm{St}+C_\parallel^{(r1)}(t_2-t_1)/\,\mathrm{St}} \\
&\quad + \frac{C_\perp^{(r1)}(\Lambda-1)e^{C_\perp^{(r1)}(t_2-t)/\,\mathrm{St}+C_\parallel^{(r1)}(t_1-t)/\,\mathrm{St}}}{C_\perp^{(r1)}+C_\parallel^{(r1)}} + \frac{C_\perp^{(r1)}(\Lambda-1)e^{C_\perp^{(r1)}(t_1-t)/\,\mathrm{St}+C_\parallel^{(r1)}(t_2-t)/\,\mathrm{St}}}{C_\perp^{(r1)}+C_\parallel^{(r1)}} \\
&\quad + \frac{C_\parallel^{(r1)}(\Lambda-1)e^{C_\parallel^{(r1)}(t_2-t_1)/\,\mathrm{St}}}{C_\perp^{(r1)}+C_\parallel^{(r1)}} + \frac{(C_\perp^{(r1)}+C_\parallel^{(r1)}\Lambda)e^{C_\perp^{(r1)}(t_2-t_1)/\,\mathrm{St}}}{C_\perp^{(r1)}+C_\parallel^{(r1)}} + e^{C_\perp^{(r1)}(-2t+t_1+t_2)/\,\mathrm{St}} + (-\Lambda-1)e^{C_\perp^{(r1)}(t_2-t)/\,\mathrm{St}} \\
d_3 &= \frac{C_\perp^{(r1)}(\Lambda-1)\Lambda e^{C_\perp^{(r1)}(t_2-t)/\,\mathrm{St}+C_\parallel^{(r1)}(t_1-t)/\,\mathrm{St}}}{C_\perp^{(r1)}+C_\parallel^{(r1)}} + \frac{\Lambda(C_\perp^{(r1)}+C_\parallel^{(r1)}\Lambda)e^{C_\perp^{(r1)}(t_2-t_1)/\,\mathrm{St}}}{C_\perp^{(r1)}+C_\parallel^{(r1)}} \\
&\quad + \Lambda e^{C_\perp^{(r1)}(-2t+t_1+t_2)/\,\mathrm{St}} - (\Lambda+1)\Lambda e^{C_\perp^{(r1)}(t_2-t)/\,\mathrm{St}} \\
d_4 &= -3\Lambda^2 e^{C_\perp^{(r1)}(t_1-t)/\,\mathrm{St}} + \Lambda^2 e^{C_\perp^{(r1)}(-2t+t_1+t_2)/\,\mathrm{St}} + \Lambda^2 e^{C_\perp^{(r1)}(t_2-t)/\,\mathrm{St}} - 2\Lambda^2 e^{C_\perp^{(r1)}(t_2-t_1)/\,\mathrm{St}} + 3\Lambda^2 \\
d_5 &= (\Lambda-1)\Lambda e^{C_\perp^{(r1)}(t_1-t)/\,\mathrm{St}+C_\parallel^{(r1)}(t_2-t_1)/\,\mathrm{St}} - \frac{C_\parallel^{(r1)}(\Lambda-1)\Lambda e^{C_\parallel^{(r1)}(t_2-t_1)/\,\mathrm{St}}}{C_\perp^{(r1)}+C_\parallel^{(r1)}}
\end{aligned}$$

$$d_6 = -\frac{C_\perp^{(r1)}(\Lambda-1)\Lambda e^{C_\perp^{(r1)}(t_1-t)/\,\mathrm{St}+C_\parallel^{(r1)}(t_2-t)/\,\mathrm{St}}}{C_\perp^{(r1)}+C_\parallel^{(r1)}} - \frac{C_\parallel^{(r1)}(\Lambda-1)\Lambda e^{C_\parallel^{(r1)}(t_2-t_1)/\,\mathrm{St}}}{C_\perp^{(r1)}+C_\parallel^{(r1)}}$$
$$+ (\Lambda-1)\Lambda e^{C_\perp^{(r1)}(t_1-t)/\,\mathrm{St}+C_\parallel^{(r1)}(t_2-t_1)/\,\mathrm{St}} + 2\Lambda e^{C_\perp^{(r1)}(t_1-t)/\,\mathrm{St}} - \Lambda e^{C_\perp^{(r1)}(-2t+t_1+t_2)/\,\mathrm{St}} + \Lambda e^{C_\perp^{(r1)}(t_2-t_1)/\,\mathrm{St}} - 2\Lambda$$

$$d_7 = 2\Lambda^2 e^{C_\perp^{(r1)}(t_1-t)/\,\mathrm{St}} - \Lambda^2 e^{C_\perp^{(r1)}(-2t+t_1+t_2)/\,\mathrm{St}} + \Lambda^2 e^{C_\perp^{(r1)}(t_2-t_1)/\,\mathrm{St}} - 2\Lambda^2$$

$$d_8 = \frac{C_\perp^{(r1)}(\Lambda-1)\Lambda e^{C_\perp^{(r1)}(t_2-t)/\,\mathrm{St}+C_\parallel^{(r1)}(t_1-t)/\,\mathrm{St}}}{C_\perp^{(r1)}+C_\parallel^{(r1)}} + \frac{\Lambda(C_\perp^{(r1)}+C_\parallel^{(r1)}\Lambda)e^{C_\perp^{(r1)}(t_2-t_1)/\,\mathrm{St}}}{C_\perp^{(r1)}+C_\parallel^{(r1)}}$$
$$+ \Lambda e^{C_\perp^{(r1)}(t_1-t)/\,\mathrm{St}} + \Lambda^2\left(-e^{C_\perp^{(r1)}(t_2-t)/\,\mathrm{St}}\right) - \Lambda$$

$$d_9 = \frac{C_\perp^{(r1)}(\Lambda-1)\Lambda e^{C_\perp^{(r1)}(t_1-t)/\,\mathrm{St}+C_\parallel^{(r1)}(t_2-t)/\,\mathrm{St}}}{C_\perp^{(r1)}+C_\parallel^{(r1)}} + \frac{C_\parallel^{(r1)}(\Lambda-1)\Lambda e^{C_\parallel^{(r1)}(t_2-t_1)/\,\mathrm{St}}}{C_\perp^{(r1)}+C_\parallel^{(r1)}}$$
$$- (\Lambda-1)\Lambda e^{C_\perp^{(r1)}(t_1-t)/\,\mathrm{St}+C_\parallel^{(r1)}(t_2-t_1)/\,\mathrm{St}} + \Lambda e^{C_\perp^{(r1)}(t_1-t)/\,\mathrm{St}} - \Lambda e^{C_\perp^{(r1)}(t_2-t)/\,\mathrm{St}} + \Lambda e^{C_\perp^{(r1)}(t_2-t_1)/\,\mathrm{St}} - \Lambda$$

$$d_{10} = \frac{(C_\perp^{(r1)}-C_\perp^{(r1)}\Lambda)e^{C_\perp^{(r1)}(t_2-t)/\,\mathrm{St}+C_\parallel^{(r1)}(t_1-t)/\,\mathrm{St}}}{C_\perp^{(r1)}+C_\parallel^{(r1)}} - \frac{(C_\perp^{(r1)}+C_\parallel^{(r1)}\Lambda)e^{C_\perp^{(r1)}(t_2-t_1)/\,\mathrm{St}}}{C_\perp^{(r1)}+C_\parallel^{(r1)}}$$
$$- e^{C_\perp^{(r1)}(t_1-t)/\,\mathrm{St}} + \Lambda e^{C_\perp^{(r1)}(t_2-t)/\,\mathrm{St}} + 1$$

$$d_{11} = -\frac{C_\perp^{(r1)}(\Lambda-1)\Lambda e^{C_\perp^{(r1)}(t_2-t)/\,\mathrm{St}+C_\parallel^{(r1)}(t_1-t)/\,\mathrm{St}}}{C_\perp^{(r1)}+C_\parallel^{(r1)}} - \frac{\Lambda(C_\perp^{(r1)}+C_\parallel^{(r1)}\Lambda)e^{C_\perp^{(r1)}(t_2-t_1)/\,\mathrm{St}}}{C_\perp^{(r1)}+C_\parallel^{(r1)}}$$
$$- \Lambda e^{C_\perp^{(r1)}(t_1-t)/\,\mathrm{St}} + \Lambda^2 e^{C_\perp^{(r1)}(t_2-t)/\,\mathrm{St}} + \Lambda$$

$$d_{12} = \Lambda^2 e^{C_\perp^{(r1)}(t_1-t)/\,\mathrm{St}} - \Lambda^2 e^{C_\perp^{(r1)}(t_2-t)/\,\mathrm{St}} + \Lambda^2 e^{C_\perp^{(r1)}(t_2-t_1)/\,\mathrm{St}} - \Lambda^2$$

$$d_{13} = \Lambda^2 e^{C_\perp^{(r1)}(t_1-t)/\,\mathrm{St}} - \Lambda^2 e^{C_\perp^{(r1)}(t_2-t)/\,\mathrm{St}} + \Lambda^2 e^{C_\perp^{(r1)}(t_2-t_1)/\,\mathrm{St}} - \Lambda^2$$

$$d_{14} = \frac{C_\perp^{(r1)}(\Lambda-1)\Lambda e^{C_\perp^{(r1)}(t_1-t)/\,\mathrm{St}+C_\parallel^{(r1)}(t_2-t)/\,\mathrm{St}}}{C_\perp^{(r1)}+C_\parallel^{(r1)}} + \Lambda\left(-e^{C_\perp^{(r1)}(t_1-t)/\,\mathrm{St}}\right) + \Lambda e^{C_\perp^{(r1)}(t_2-t)/\,\mathrm{St}} - \Lambda e^{C_\perp^{(r1)}(t_2-t_1)/\,\mathrm{St}} + \Lambda$$

$$d_{15} = \Lambda^2\left(-e^{C_\perp^{(r1)}(t_1-t)/\,\mathrm{St}}\right) + \Lambda^2 e^{C_\perp^{(r1)}(t_2-t)/\,\mathrm{St}} - \Lambda^2 e^{C_\perp^{(r1)}(t_2-t_1)/\,\mathrm{St}} + \Lambda^2$$

where $\Lambda = (\lambda^2-1)/(\lambda^2+1)$, $C_\perp^{(r1)} \equiv 5K_\perp^{(r1)}/(a_\parallel^2+a_\perp^2)$, and $C_\parallel^{(r1)} \equiv 5K_\parallel^{(r1)}/(2a_\perp^2)$. To obtain the first term in the last row of Eq. (3) in the main text, for example, we must add the terms involving d_1, d_2, and d_{10}.

C. Moments of alignment

Eq. (S17) relates the orientation dynamics to the fluid velocity and its gradients. This expression makes it possible to calculate the moments $\langle(\boldsymbol{n}\cdot\hat{\boldsymbol{g}})^{2p}\rangle_{\boldsymbol{n}_0}$ conditional on $\boldsymbol{n}_0$ (odd-order moments vanish because spheroids are fore-aft symmetric). By raising Eq. (S17) to the power $2p$, terminating the resulting expressions at order Ku^2, and taking the average using the known stationary statistics of the fluid velocity and its gradients, we obtain the moments of $\boldsymbol{n}\cdot\hat{\boldsymbol{g}}$ conditional on initial alignment $\boldsymbol{n}_0\cdot\hat{\boldsymbol{g}}$.

However, the resulting expressions contain secular terms. These terms are proportional to Ku^2 and grow linearly with time. We know that such secular terms must vanish, because the vector $\boldsymbol{n}$ must remain normalised to unity. Its components cannot continue to grow. We therefore demand that the initial alignment $\boldsymbol{n}_0\cdot\hat{\boldsymbol{g}}$ is distributed according to a stationary distribution of alignments that causes all secular terms to vanish. This procedure gives rise to one condition per value of p, and this is sufficient to determine the desired stationary distribution of alignments.

The dependence of the secular terms upon $(\boldsymbol{n}_0\cdot\hat{\boldsymbol{g}})^{2p}$ is not only through algebraic powers, but also functional through exponentials and error functions. As a consequence, the conditions that make sure that the secular terms vanish are hard to solve in general. We therefore seek a perturbative solution and expand the secular conditions and

the moments $m_p \equiv \langle(\boldsymbol{n}_0 \cdot \hat{\boldsymbol{g}})^{2p}\rangle$ in terms of the parameter $G \equiv \mathrm{Ku}\, F/C_\perp^{(t)}$, for instance:

$$m_p = \sum_{i=0}^{\infty} m_p^{(i)} G^i \,. \tag{S18}$$

To lowest order in G we find the recursion

$$(1+2p)m_p^{(0)} + (1-2p)m_{p-1}^{(0)} = 0\,. \tag{S19}$$

Using the boundary condition $m_0^{(0)} = 1$ we find

$$m_p^{(0)} = \frac{1}{2p+1}\,. \tag{S20}$$

These moments correspond to a uniform distribution of $\boldsymbol{n}_0$. Higher-order contributions in G to the moments can be recursively determined by series expansion of the secular terms. We find that moments $m_p^{(i)}$ with odd values of i vanish, and that moments $m_p^{(i)}$ with even values of i are on the form given by Eq. (6) in the main article:

$$\langle(\boldsymbol{n}\cdot\hat{\boldsymbol{g}})^{2p}\rangle_\infty = \frac{1}{2p+1} + \sum_{i=1}^{\infty} \frac{\mathrm{G}^{2i}\sum_{j=1}^{i} p^j A_j^{(2i)}(\mathrm{St},\lambda)}{\prod_{k=1}^{i+1}(2p+2k-1)}\,. \tag{S21}$$

The coefficients $A_j^{(2i)}(\mathrm{St},\lambda)$ are quite lengthy in general. We therefore only give the lowest-order expression here. To order G^2 we have

$$\langle(\boldsymbol{n}\cdot\hat{\boldsymbol{g}})^{2p}\rangle_\infty = \frac{1}{2p+1} + \frac{\mathrm{G}^2\, p A_1^{(2)}(\mathrm{St},\lambda)}{(2p+1)(2p+3)}\,. \tag{S22}$$

Decomposing $A_1^{(2)}(\mathrm{St},\lambda)$ in one contribution due to preferential sampling and one due to the history effect, we have

$$A_1^{(2)}(\mathrm{St},\lambda) = A_{1,\mathrm{pref.}}^{(2)}(\mathrm{St},\lambda) + A_{1,\mathrm{hist.}}^{(2)}(\mathrm{St},\lambda)\,. \tag{S23}$$

The preferential-sampling contribution reads:

$$A_{1,\mathrm{pref.}}^{(2)}(\mathrm{St},\lambda) = \frac{7-\Lambda}{5+3\Lambda^2}\,\frac{4C_\perp^{(t)}\,\mathrm{St}^3(C_\perp^{(t)}-C_\parallel^{(t)})\Big[\big(C_\perp^{(t)}\big)^2+\big(C_\parallel^{(t)}\big)^2+C_\perp^{(t)}C_\parallel^{(t)}+3\,\mathrm{St}\,\big(C_\perp^{(t)}+C_\parallel^{(t)}+3\,\mathrm{St}\,\big)\Big]}{3(C_\perp^{(t)}+\mathrm{St})^3 C_\parallel^{(t)}(C_\parallel^{(t)}+\mathrm{St})^3}\,. \tag{S24}$$

The contribution due to the history effect is

$$\begin{aligned}
A_{1,\mathrm{history}}^{(2)}(\mathrm{St},\lambda) = {}& \frac{1}{3{C_\parallel^{(t)}}^2\,(3\Lambda^2+5)\,(10C_\parallel^{(t)}+3\mathrm{St})^3(10C_\perp^{(t)}C_\parallel^{(t)}-3C_\perp^{(t)}\mathrm{St}+6C_\parallel^{(t)}\mathrm{St})^3}\Big[\\
&-2000000\,{C_\perp^{(t)}}^3{C_\parallel^{(t)}}^6\Big(-4{C_\perp^{(t)}}^2\big(4\Lambda^2+7\Lambda+7\big)+C_\perp^{(t)}C_\parallel^{(t)}\big(3\Lambda^2+28\Lambda-7\big)+{C_\parallel^{(t)}}^2\big(19\Lambda^2-42\Lambda+35\big)\Big)\\
&-3600000\,\mathrm{St}{C_\perp^{(t)}}^2{C_\parallel^{(t)}}^6\Big(-4{C_\perp^{(t)}}^2\big(4\Lambda^2+7\Lambda+7\big)+C_\perp^{(t)}C_\parallel^{(t)}\big(3\Lambda^2+28\Lambda-7\big)+{C_\parallel^{(t)}}^2\big(19\Lambda^2-42\Lambda+35\big)\Big)\\
&-540000\,\mathrm{St}^2C_\perp^{(t)}{C_\parallel^{(t)}}^4\Big({C_\perp^{(t)}}^2-2C_\perp^{(t)}C_\parallel^{(t)}-4{C_\parallel^{(t)}}^2\Big)\Big(4{C_\perp^{(t)}}^2\big(4\Lambda^2+7\Lambda+7\big)+C_\perp^{(t)}C_\parallel^{(t)}\big(-3\Lambda^2-28\Lambda+7\big)\\
&\qquad+{C_\parallel^{(t)}}^2\big(-19\Lambda^2+42\Lambda-35\big)\Big)\\
&-108000\,\mathrm{St}^3{C_\parallel^{(t)}}^4\Big(7{C_\perp^{(t)}}^4\big(15\Lambda^2+22\Lambda+23\big)-21{C_\perp^{(t)}}^3C_\parallel^{(t)}\big(11\Lambda^2+24\Lambda+13\big)-4{C_\perp^{(t)}}^2{C_\parallel^{(t)}}^2\big(32\Lambda^2-119\Lambda+105\big)\\
&\qquad+8C_\perp^{(t)}{C_\parallel^{(t)}}^3\big(30\Lambda^2-49\Lambda+49\big)+4{C_\parallel^{(t)}}^4\Big(19\Lambda^2-42\Lambda+35\big)\Big)\\
&-48600\,\mathrm{St}^4{C_\parallel^{(t)}}^2\Big({C_\perp^{(t)}}^5\big(-\big(23\Lambda^2+28\Lambda+21\big)\big)+14{C_\perp^{(t)}}^4C_\parallel^{(t)}\big(7\Lambda^2+12\Lambda+5\big)+{C_\perp^{(t)}}^3{C_\parallel^{(t)}}^2\big(-41\Lambda^2-210\Lambda+119\big)\\
&\qquad-8{C_\perp^{(t)}}^2{C_\parallel^{(t)}}^3\big(22\Lambda^2+7\Lambda+49\big)+8C_\perp^{(t)}{C_\parallel^{(t)}}^4\big(3\Lambda^2+28\Lambda-7\big)+8{C_\parallel^{(t)}}^5\big(19\Lambda^2-42\Lambda+35\big)\Big)\\
&+29160\,\mathrm{St}^5{C_\parallel^{(t)}}^2(C_\perp^{(t)}-2C_\parallel^{(t)})^2\Big(14{C_\perp^{(t)}}^2\big(\Lambda^2+3\Lambda+2\big)+C_\perp^{(t)}C_\parallel^{(t)}\big(-3\Lambda^2-28\Lambda+7\big)+{C_\parallel^{(t)}}^2\big(-19\Lambda^2+42\Lambda-35\big)\Big)\\
&-1458\,\mathrm{St}^6(C_\perp^{(t)}-2C_\parallel^{(t)})^3\Big({C_\perp^{(t)}}^2\big(9\Lambda^2+28\Lambda+35\big)+{C_\parallel^{(t)}}^2\big(-19\Lambda^2+42\Lambda-35\big)\Big)\Big]\,.
\end{aligned} \tag{S25}$$

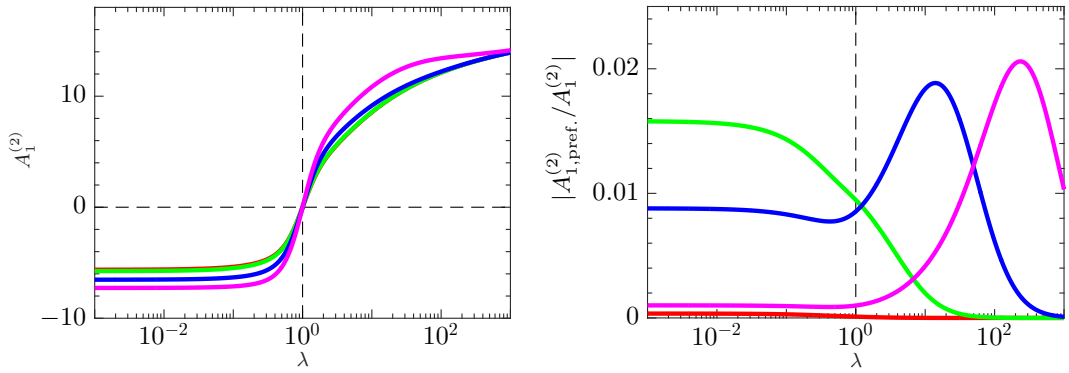

FIG. S2: Left: Coefficient $A_1^{(2)}(\mathrm{St},\lambda)$ [Eqs. (S23)–(S25)] plotted against λ for St = 0.1 (red), 1 (green), 10 (blue), 100 (magenta). Right: Corresponding plot for the relative contribution due to preferential sampling $|A_{1,\mathrm{pref.}}^{(2)}(\mathrm{St},\lambda)/A_1^{(2)}(\mathrm{St},\lambda)|$.

Here we have used the identities

$$C_\perp^{(r1)} = \frac{10}{3} C_\parallel^{(t)} \quad \text{and} \quad C_\parallel^{(r1)} = \frac{10}{3} \frac{C_\perp^{(t)} C_\parallel^{(t)}}{2C_\parallel^{(t)} - C_\perp^{(t)}} \tag{S26}$$

to simplify. Eq. (S4) relates $C_\perp^{(t)}$ and $C_\parallel^{(t)}$ to λ, so that $A_1^{(2)}$ is a function of St and λ only. Fig. S2 shows how the expressions for $A_1^{(2)}$ and for the relative preferential-sampling contribution $|A_{1,\mathrm{pref.}}^{(2)}/A_1^{(2)}|$ depend on the aspect ratio λ, for different values of St. We see that the preferential contribution is small compared to the contribution due to the history effect for all parameter values.

D. *Large-*G *limit*

In the previous Section we summarised how the moments of the orientation distribution can be calculated by using perturbation expansions in the parameter G. Now consider the opposite limit of large values of G. In this limit we obtain a recursion equation for the moments $\langle(\boldsymbol{n}\cdot\hat{\boldsymbol{g}})^{2p}\rangle$ that is independent of preferential effects. This is expected because the particles fall rapidly through the turbulence in this limit, experiencing the turbulent gradients approximately as a white-noise signal. The history contribution is obtaind from a fourth-order recursion that is hard to solve in general.

One might expect that the orientation of rod-like particles approaches perfect alignment with gravity, that is $\langle(\boldsymbol{n}\cdot\hat{\boldsymbol{g}})^{2p}\rangle = 1$ for all values of p as $G\to\infty$. However, when we insert this limiting expression into the fourth-order recursion equation, we obtain a condition that is only satisfied when $\lambda=\infty$. This shows that perfect alignment is only possible when $\lambda=\infty$. For other values of λ the moments must approach limiting values as $G\to\infty$. We have not yet managed to calculate these limits from our statistical-model theory.

[1] S. Kim and S. J. Karrila, *Microhydrodynamics: principles and selected applications* (Butterworth-Heinemann, Boston, 1991).
[2] L. D. Landau and E. M. Lifshitz, *Mechanics* (Pergamon Press Ltd., Oxford, 1969).
[3] M. Voßkuhle, A. Pumir, E. Lévêque, and M. Wilkinson, J. Fluid Mech. **749**, 841 (2014).
[4] S. A. Orszag, J. Atmos. Sci. **28** (1971).
[5] H. R. Pruppacher and J. D. Klett, *Microphysics of clouds and precipitation, 2nd edition* (Kluwer Academic Publishers, Dordrecht, The Nederlands, 1997), 954p.
[6] K. Gustavsson and B. Mehlig, Adv. Phys. **65**, 1 (2016).